Generating Entangled Two-Photon States with Coincident Frequencies

Vittorio Giovannetti, Lorenzo Maccone, Jeffrey H. Shapiro, and Franco N. C. Wong
Massachusetts Institute of Technology, Research Laboratory of Electronics, Cambridge, Massachusetts 02139
(Received 26 September 2001; published 17 April 2002)

It is shown that parametric down-conversion, with a short-duration pump pulse and a long nonlinear crystal that is appropriately phase matched, can produce a frequency-entangled biphoton state whose individual photons are coincident in frequency. Quantum interference experiments which distinguish this state from the familiar time-coincident biphoton state are described.

DOI: 10.1103/PhysRevLett.88.183602 PACS numbers: 42.50.Dv, 03.65.Ud, 03.67.–a, 42.25.Hz

Spontaneous parametric down-conversion (SPDC) has been the entanglement source of choice for experimental demonstrations of quantum teleportation, entanglement-based quantum cryptography, Bell-inequality violations, etc. However, the biphoton state generated via SPDC under the customary phase-matching conditions is maximally entangled only when a continuous-wave (cw) pump is used [1,2]. In pulsed-pump experiments, the fringe visibility in biphoton interference measurements decreases as the duration of the pump pulse is reduced [3]. The timing and pump-intensity advantages of pulsed experiments has thus spurred work to retain or restore maximal entanglement in the pulsed regime [4].

In this paper a new method for obtaining maximal entanglement from pulsed SPDC is reported. Our approach uses a long nonlinear crystal and extended phase-matching conditions tailored specifically to pulsed operation. As such, it does not require any filtering or postselection, and it reaps the high-conversion-efficiency advantage that long crystals afford. Furthermore, the biphoton states that it produces are comprised of photons that are coincident in frequency, in contrast to the usual cw phase-matching case whose biphotons exhibit coincidence in time. Coincident-in-frequency entanglement is important because the N-photon version of such a state has been shown to improve the accuracy of time-of-flight position sensing or clock synchronization by a factor of $\sqrt{N}$ [5].

Consider SPDC with a cw pump and conventional phase matching that is operated at frequency degeneracy, i.e., phase matched such that the center frequencies of its signal and idler equal half the pump frequency. This system produces a biphoton of the form

$$|\mathrm{TB}\rangle \equiv \int \frac{d\omega}{2\pi}\, \phi(\omega)\, |\omega_p/2 - \omega\rangle_s |\omega_p/2 + \omega\rangle_i\,. \quad (1)$$

Here, $|\omega_s\rangle_s$ and $|\omega_i\rangle_i$ are single-photon signal and idler states in which the photons are present at frequencies ω_s and ω_i, respectively; ω_p is the pump frequency; and $\phi(\omega)$ is the spectral function of the state, so that $|\phi(\omega_p/2 - \omega)|^2$ is the signal's fluorescence spectrum. The notation $|\mathrm{TB}\rangle$ indicates that Eq. (1) is the usual twin-beam state of SPDC. The frequency entanglement of this state dictates that a signal photon at frequency $\omega_p/2 - \omega$ is accompanied by an idler photon at frequency $\omega_p/2 + \omega$. The sum of the signal and idler frequencies is therefore fixed at the pump frequency. By Fourier duality, this implies that the signal and idler photons occur in time coincidence—to within a reciprocal fluorescence bandwidth—as has been shown in the famous "Mandel dip" experiment [6].

On the other hand, the SPDC biphoton that will be studied in this paper is

$$|\mathrm{DB}\rangle = \int \frac{d\omega}{2\pi}\, \phi(\omega)\, |\omega_p/2 + \omega\rangle_s |\omega_p/2 + \omega\rangle_i\,. \quad (2)$$

In this state, a signal photon at $\omega_p/2 + \omega$ is accompanied by an idler photon at the same frequency. This coincident-in-frequency behavior leads, via Fourier duality, to symmetrically located occurrences in time. In particular, a signal photon appearing at $T_0 + t$ is accompanied by an idler photon at $T_0 - t$, where T_0 is the mean time of arrival of the biphoton pulse. Because this biphoton possesses a narrow distribution in signal-minus-idler difference frequency, we have dubbed it the difference-beam ($|\mathrm{DB}\rangle$) state. Note that its mean time of arrival, T_0, plays the role of the fluorescence center frequency, $\omega_p/2$, in comparing the DB and TB states. Thus, whereas the photons in $|\mathrm{TB}\rangle$ may be discriminated by frequency measurements, those in $|\mathrm{DB}\rangle$ may be distinguished via time-of-arrival measurements.

The rest of the paper is organized as follows. First, we derive the output state of SPDC. The phase-matching conditions that are needed to create the DB state are then obtained and explained. Next, we present quantum interference experiments that can distinguish between the TB and the DB states. Finally, we give a feasibility study for $|\mathrm{DB}\rangle$ generation using periodically poled potassium titanyl phosphate (PPKTP).

A textbook treatment of the SPDC process (see, for example, [7]) allows us to deduce the state at the output of a compensated SPDC crystal. We will give a brief derivation here assuming colinear plane-wave operation. In the interaction picture under the rotating-wave approximation, the Hamiltonian that gives rise to the creation of the two down-converted photons starting from a single pump photon is given by

$$H_I(t) = S \int_{-L/2}^{L/2} dz\, \chi^{(2)} E_p^{(+)}(z,t) E_s^{(-)}(z,t) \times E_i^{(-)}(z,t) + \text{H.c.}, \quad (3)$$

where $\chi^{(2)}$ is the nonlinear coefficient and L is the length of the down-conversion crystal, S is the pump-beam area, and $E^{(+)}$ and $E^{(-)} \equiv (E^{(+)})^\dagger$ are positive-frequency and negative-frequency electric field operators with the subscripts $\{p, s, i\}$ denoting pump, signal, and idler, respectively. These electric field operators obey

$$E_j^{(+)}(z,t) = i \int \frac{d\omega}{2\pi} \sqrt{\frac{\pi\hbar\omega}{c\epsilon_0 n_j^2(\omega) S}}\, a_j(\omega) e^{i[k_j(\omega)z - \omega t]}, \quad (4)$$

for $j = p, s, i$, where $a_j(\omega)$ is the annihilation operator for frequency-ω photons, $n_j(\omega)$ is the refractive index for the jth beam (pump, signal, or idler), and $k_j(\omega) \equiv \omega n_j(\omega)/c$ is the associated wave number.

The Hamiltonian (3) yields the state at the output of the crystal (for vacuum-input signal and idler) via

$$|\Psi\rangle \simeq |0\rangle - \frac{i}{\hbar} \int_{t_0}^{t} dt'\, H_I(t') |0\rangle, \quad (5)$$

for small values of the coupling constant $\chi^{(2)}$. As done in [2], we shall assume that $\chi^{(2)}$ is independent of frequency over the pump bandwidth, even though this assumption may not be satisfied in some ultrafast applications. For a strong coherent pump pulse and in the absence of pump depletion, we may replace the pump field operator in Eq. (3) with

$$E_p^{(+)}(z,t) \simeq \int \frac{d\omega}{2\pi}\, \mathcal{E}_p(\omega) e^{i[k_p(\omega)z - \omega t]}, \quad (6)$$

where $\mathcal{E}_p(\omega)$ is a classical complex amplitude. Because we are interested in the fields far from the crystal, we may expand the integration limits in Eq. (5) to run from $-\infty$ to $+\infty$. Thus, the t' integration produces an impulse, $\delta(\omega_p - \omega_s - \omega_i)$, that expresses energy conservation at the photon level.

The biphoton state that we are seeking is the nonvacuum part of Eq. (5). Under the preceding assumptions, this is given by

$$|\Psi\rangle = i \frac{\chi^{(2)}\pi}{c\epsilon_0} \int \frac{d\omega_s}{2\pi} \int \frac{d\omega_i}{2\pi}\, \alpha(\omega_s, \omega_i) \times \Phi_L(\omega_s, \omega_i) |\omega_s\rangle_s |\omega_i\rangle_i, \quad (7)$$

where $|\omega\rangle \equiv a^\dagger(\omega)|0\rangle$ is a single-photon state,

$$\alpha(\omega_s, \omega_i) \equiv \frac{\sqrt{\omega_s \omega_i}}{n_s(\omega_s) n_i(\omega_i)}\, \mathcal{E}_p(\omega_s + \omega_i) \quad (8)$$

is determined by the pump spectrum, and

$$\Phi_L(\omega_s, \omega_i) \equiv \frac{\sin[\Delta k(\omega_s, \omega_i) L/2]}{\Delta k(\omega_s, \omega_i)/2} \quad (9)$$

is the phase-matching function, with $\Delta k(\omega_s, \omega_i) \equiv k_p(\omega_s + \omega_i) - k_s(\omega_s) - k_i(\omega_i)$.

To obtain maximal entanglement from the biphoton state (7), we need to collapse the double integral over frequency into a single integral. For the customary twin-beam state $|\text{TB}\rangle$, this is accomplished by using a cw pump of frequency ω_p to force $\alpha(\omega_s, \omega_i) \propto \delta(\omega_s + \omega_i - \omega_p)$ in Eq. (7). We then obtain a TB state (1) with spectral function $\phi(\omega) \propto \Phi_L(\omega_p/2 - \omega, \omega_p/2 + \omega)$. Because this makes the common signal/idler fluorescence bandwidth, Ω_f, inversely proportional to L, it follows that short crystals are better suited to generating broadband TB states. For DB states, however, we will see that long crystals do not prevent broadband entanglement generation.

Continuous-wave operation is not the only way to obtain a maximally entangled state from (7). We can also eliminate one of the frequency integrals by forcing Φ_L to approach a delta function. The property $\lim_{L\to\infty}[\sin(xL)/x] = \pi\delta(x)$ allows us to write $\Phi_L(\omega_s, \omega_i) = 2\pi\delta(\Delta k(\omega_s, \omega_i))$ for an infinitely long crystal. (In practice, the nonlinear crystal will always have a finite length L, but we will see that a high degree of entanglement can be obtained using practical values of L.) To force $\Phi_L(\omega_s, \omega_i) \propto \delta(\omega_s - \omega_i)$ in the long-crystal limit, we need to ensure that $\Delta k(\omega_s, \omega_i) = 0$ if and only if $\omega_s = \omega_i$, for $\omega_s + \omega_i$ ranging over the full pump bandwidth, Ω_p. Equation (7) then reduces to the DB state of Eq. (2), with spectral function $\phi(\omega) = \alpha(\omega_p/2 + \omega, \omega_p/2 + \omega)$, where ω_p is the pump beam's center frequency. Note that $\phi(\omega)$ depends only on the pump spectrum and the refractive indexes of the nonlinear crystal, as can be seen from Eq. (8), and that its bandwidth is $\Omega_p/2$. Moreover, the symmetry of the phase-matching function Φ_L forces the signal and idler fluorescence spectra to be identical, something that is not generally true in ultrafast type-II down-conversion [2].

Is it possible to satisfy the condition $\Delta k(\omega_s, \omega_i) = 0$ only for $\omega_s = \omega_i$ over the full pump bandwidth? What does this condition correspond to physically? By using the first-order Taylor expansions of k_s and k_i around $\omega_p/2$ and of k_p around ω_p, we find that

$$n_p(\omega_p) = \frac{n_s(\omega_p/2) + n_i(\omega_p/2)}{2}, \quad (10)$$

$$k_p'(\omega_p) = \frac{k_s'(\omega_p/2) + k_i'(\omega_p/2)}{2} \quad (11)$$

ensure that $\Delta k(\omega_p/2 + \omega, \omega_p/2 + \omega) = 0$ for $|\omega| \le \Omega_p/2$. In physical terms, the extended phase-matching condition given by (10) and (11) assert that the index of refraction and the inverse group velocity seen by the pump must equal the averages of those seen by the signal and idler. Equation (10) is the customary phase-matching condition required for the generation of $|\text{TB}\rangle$ at frequency degeneracy. Equation (11) is equivalent to the "group velocity matching" condition introduced in [3]. It turns out, however, that Eqs. (10) and (11) are not sufficient for DB state generation. Because $\Delta k(\omega_s, \omega_i)$ must vanish

only for $\omega_s = \omega_i$, we must also require that $k_s'(\omega_p/2) \neq k_i'(\omega_p/2)$. This requirement excludes type-I crystals, for which $k_s(\omega) = k_i(\omega)$. Thus, in all that follows we will presume type-II operation. We will discuss later the validity of truncating the Taylor series at the $n = 1$ terms.

The states $|\mathrm{DB}\rangle$ and $|\mathrm{TB}\rangle$ are duals in the following sense. The former is a biphoton whose constituent photons are coincident in frequency, and the latter is a biphoton whose constituent photons are time coincident. We now show that coincidence counting using Hong-Ou-Mandel (HOM) and Mach-Zehnder (MZ) interferometers, as sketched in Fig. 1, can provide experimental quantum-interference signatures that distinguish between the TB and DB biphoton states.

To understand the outcome of the two experiments shown in Fig. 1, it is useful to start from the general state $|\Psi\rangle$ of the form (7). The coincidence rate for detection intervals that are long compared to the reciprocal fluorescence bandwidth is given by (see, for example, [1,2])

$$P \propto \int \frac{d\omega_1}{2\pi} \int \frac{d\omega_2}{2\pi} |\langle 0|a_1(\omega_1)a_2(\omega_2)|\Psi\rangle|^2, \quad (12)$$

where a_1 and a_2 are the photon annihilation operators at the two detectors and $|\Psi\rangle$ is the biphoton state of the source. Assume that the product $\alpha(\omega_1, \omega_2)\Phi_L(\omega_1, \omega_2)$ is symmetric in ω_1, ω_2, as is the case for both $|\mathrm{TB}\rangle$ and $|\mathrm{DB}\rangle$. By applying the beam-splitter transformations on the operators a_s and a_i, we find that

$$P_{\pm}(\tau) \propto \int \frac{d\omega_1}{2\pi} \int \frac{d\omega_2}{2\pi} |\alpha(\omega_1, \omega_2)\Phi_L(\omega_1, \omega_2)|^2 \times \{1 \pm \cos[(\omega_1 \pm \omega_2)\tau]\}. \quad (13)$$

In (13), the minus signs apply to the HOM interferometer, and the plus signs apply to the MZ interferometer.

For the TB state, we set $|\alpha(\omega_1, \omega_2)|^2 \propto \delta(\omega_p - \omega_1 - \omega_2)$ and $|\Phi_L(\omega_1, \omega_2)|^2 \propto |\phi[(\omega_2 - \omega_1)/2]|^2$. Approximating the fluorescence spectrum by $|\phi(\omega)|^2 = \sin^2(2\pi\omega/\Omega_f)/[2\pi\omega/(\Omega_f L)]^2$, where $\Omega_f \equiv 4\pi/(L|k_s'(\omega_p/2) - k_i'(\omega_p/2)|)$, Eq. (13) then yields the familiar triangular-shaped HOM coincidence dip of width $4\pi/\Omega_f$ centered at $\tau = 0$ [1,2]. The $|\mathrm{TB}\rangle$ coincidences require that one photon exits from each output port of the beam splitter. At zero relative delay, the two quantum trajectories that give rise to such coincidences destructively interfere, leading to a coincidence null [8]. The width of this dip is $\sim 1/\Omega_f$, because signal and idler wave packets separated by many reciprocal fluorescence bandwidths are distinguishable and, hence, do not interfere. When the TB-state coincidence rate is evaluated for the MZ interferometer, we obtain $P_+(\tau) \propto 1 + \cos(\omega_p\tau)$, i.e., sinusoidal fringes at the pump frequency. These fringes have an infinite extent because a perfect cw pump has an infinite coherence time.

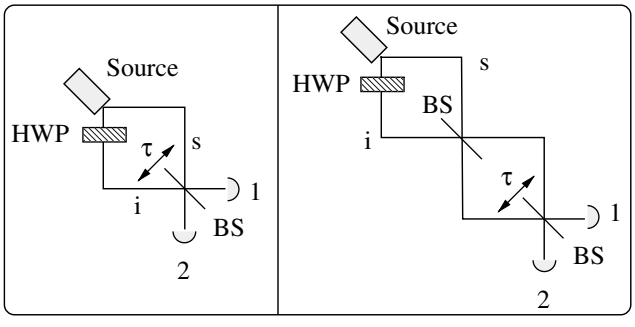

FIG. 1. Quantum interference experiments to distinguish $|\mathrm{DB}\rangle$ from $|\mathrm{TB}\rangle$. The left panel shows the HOM interferometer and the right shows the MZ interferometer. In both cases, coincidence counts are measured as the relative delay, τ, between the interferometer's arms is varied by moving the beam splitter that is nearest to the detectors. The half-wave plate rotates the idler polarization to match that of the signal because type-II down-conversion is assumed.

Now suppose that the input state in Fig. 1 is $|\mathrm{DB}\rangle$, i.e., let $|\Phi_L(\omega_1, \omega_2)|^2 \propto \delta(\omega_1 - \omega_2)$ and $|\alpha(\omega_1, \omega_2)|^2 = |\phi[(\omega_1 + \omega_2 - \omega_p)/2]|^2$ in Eq. (13). In this case, the frequency coincidence between the signal and idler photons eliminates any delay dependence in the HOM configuration, reducing Eq. (13) to $P_-(\tau) = 0$. In fact, the wave functions for the two photons extend to all times and cannot be separated: The quantum trajectories that give rise to coincidences destructively interfere for any delay τ. For the Mach-Zehnder arrangement, the DB state gives $P_+(\tau) \propto 1 + \exp(-\Omega_p^2\tau^2/4)\cos(\omega_p\tau)$, under the assumption of Gaussian pump spectrum $|\phi(\omega)|^2 \propto \exp[-4\omega^2/\Omega_p^2]$. Notice that in this case P_+ again exhibits pump-frequency interference fringes, but now the interference pattern has width $4/\Omega_p$, i.e., roughly equal to the duration of a transform-limited pump pulse. Similar interference patterns have been previously analyzed in [9].

Both the HOM and the MZ interferometers distinguish between the states $|\mathrm{DB}\rangle$ and $|\mathrm{TB}\rangle$. However, because DB state generation requires infinite crystal length—whereas TB state generation uses a finite-length crystal—it behooves us to study what happens in the finite-L regime when we use a pulsed pump in conjunction with our extended phase-matching conditions. The biphoton state, $|\mathrm{DB}_L\rangle$, that this system generates is entangled in frequency, but not maximally so, i.e., measuring the frequency of the signal photon does not exactly determine the frequency of the idler photon. When $|\mathrm{DB}_L\rangle$ is measured with an HOM interferometer, the resulting coincidence null is no longer of unlimited extent. Indeed, the width of the coincidence dip for $|\mathrm{DB}_L\rangle$ is identical to that for $|\mathrm{TB}\rangle$. Thus the HOM interferometer cannot distinguish between these two states. The MZ interferometer, however, does distinguish between $|\mathrm{DB}_L\rangle$ and $|\mathrm{TB}\rangle$, as the width of the former's fringe pattern is set by the pump bandwidth and, hence, independent of crystal length.

More insight into the complementary behavior of $|\mathrm{TB}\rangle$ and $|\mathrm{DB}\rangle$ can be gained by examining their time domain structures. Both of these biphoton states arise from the coherent superposition of spatially localized, instantaneous

signal/idler pair creations occurring throughout the length of the nonlinear crystal. HOM and MZ interferometers use integrating photodetectors, but reveal temporal aspects of $|\mathrm{TB}\rangle$ and $|\mathrm{DB}\rangle$ via quantum interference. Suppose, however, that we use an ultrafast photodetector to measure the arrival time of the signal photon. This measurement specifies a definite location, along the crystal, at which the detected signal photon was created, and implies rather different temporal statistics for its associated idler photon depending on whether the biphoton was $|\mathrm{TB}\rangle$ or $|\mathrm{DB}\rangle$. Because the TB state is produced by a cw pump, its component photons may be created at any time. However, once its signal photon has been detected at time T_s, the accompanying idler photon must be at T_i, where $|T_s - T_i| \leq 4\pi/\Omega_f$ for our type-II system. The individual photons in the DB state also may be created at any time, even though this biphoton is generated by a pulsed pump. Here, the timing uncertainty is really uncertainty in the location, within the infinitely long crystal, at which the photon pair is generated. Once again, detection of a signal photon at time T_s provides location information which strongly constrains the arrival time for the idler photon. In particular, the extended phase-matching conditions that produce the DB state under pulsed pumping force $(T_s + T_i)/2$ to have a mean value at a fixed offset (set by dispersion) from the peak of the classical Gaussian pump pulse.

It turns out to be difficult to find a crystal satisfying the two conditions (10) and (11). Thus, we will enforce (10) via quasi phase matching in a periodically poled $\chi^{(2)}$ material [10], i.e., one for which the addition of an artificial grating results in a spatially varying nonlinear coefficient, $\chi^{(2)}(z) = \chi^{(2)} \exp(i2\pi z/\Lambda)$, along the propagation axis. By choosing the grating period Λ to cancel the zeroth-order term in the $\Delta k(\omega_s, \omega_i)$ expansion, we can replace Eq. (10) with the new condition $n_p(\omega_p) = [n_s(\omega_p/2) + n_i(\omega_p/2)]/2 - 2\pi c/(\Lambda\omega_p)$. This, together with Eq. (11), is satisfied by PPKTP at a pump wavelength of 790 nm with a grating period of 47.7 μm when propagation is along the crystal's X axis, the pump and idler are Y polarized, and the signal is Z polarized. It still remains for us to examine the validity conditions for the $L \to \infty$ approximation to the phase-matching function $\Phi_L(\omega_s, \omega_i)$. These can be shown to be $2\pi/\gamma\Omega_p \ll L \ll 8\pi/\mu\Omega_p^2$, where $\gamma \equiv |k_p'(\omega_p) - k_s'(\omega_p/2)|$, and μ is the maximum-magnitude eigenvalue of the Hessian matrix associated with the 2D Taylor series expansion of $\Delta k(\omega_s, \omega_i)$. Physically, the lower limit on crystal length is set by our need to be in the long-L regime, and the upper limit is set by the second-order terms in the Taylor expansion. For our PPKTP example, we have that $\gamma \approx 1.4 \times 10^{-4}$ ps/μm and $\mu \approx 3.6 \times 10^{-7}$ ps^2/μm. With a 170 fs ($\Omega_p/2\pi = 3$ THz) transform-limited pump pulse, the preceding crystal-length restrictions reduce to 0.23 cm $\ll L \ll$ 19.7 cm, so that a 2-cm-long crystal will suffice. Finally, we note that polarization-entangled DB states can be created by paralleling the procedure in [11] for the creation of polarization-entangled TB states.

This work was funded by the ARO under a MURI program (Grant No. DAAD 19-00-1-0177) and by the NRO.

[1] M. H. Rubin, D. N. Klyshko, Y. H. Shih, and A. V. Sergienko, Phys. Rev. A **50**, 5122 (1994).
[2] W. P. Grice and I. A. Walmsley, Phys. Rev. A **56**, 1627 (1997).
[3] T. E. Keller and M. H. Rubin, Phys. Rev. A **56**, 1534 (1997).
[4] G. Di Giuseppe, L. Haiberger, F. De Martini, and A. V. Sergienko, Phys. Rev. A **56**, R21 (1997); A. V. Sergienko *et al., ibid.* **60**, R2622 (1999); D. Branning, W. Grice, R. Erdmann, and I. A. Walmsley, *ibid.* **62**, 013814 (2000); Y.-H. Kim, S. P. Kulik, and Y. Shih, *ibid.* **62**, 011802(R) (2000).
[5] V. Giovannetti, S. Lloyd, and L. Maccone, Nature (London) **412**, 417 (2001); Phys. Rev. A **65**, 022309 (2002).
[6] C. K. Hong, Z. Y. Ou, and L. Mandel, Phys. Rev. Lett. **59**, 2044 (1987).
[7] L. Mandel and E. Wolf, *Optical Coherence and Quantum Optics* (Cambridge University Press, Cambridge, England, 1995), Chap. 22.4.
[8] T. B. Pittman *et al.,* Phys. Rev. Lett. **77**, 1917 (1996).
[9] T. S. Larchuk *et al.,* Phys. Rev. Lett. **70**, 1603 (1993); J. H. Shapiro and K.-X. Sun, J. Opt. Soc. Am. B **11**, 1130 (1994); Y. H. Shih *et al.,* Phys. Rev. A **49**, 4243 (1994); D. Branning, A. L. Migdall, and A. V. Sergienko, *ibid.* **62**, 063808 (2000).
[10] M. M. Fejer, G. A. Magel, D. H. Jundt, and R. L. Byer, IEEE J. Quantum Electron. **28**, 2631 (1992).
[11] J. H. Shapiro and N. C. Wong, J. Opt. B **2**, L1 (2000).